Extended x-ray-absorption fine-structure and near-edge-structure studies on evaporated small clusters of Au

A. Balerna, E. Bernieri, P. Picozzi, A. Reale, and S. Santucci
Istituto di Fisica, Università de L'Aquila, L'Aquila, Italy

E. Burattini
Consiglio Nazionale delle Ricerche and Istituto Nazionale di Física Nucleare, Laboratori Nazionali di Frascati, 00044 Frascati, Italy

S. Mobilio
Istituto Nazionale di Física Nucleare, Laboratori Nazionali Frascati, 00044 Frascati, Italy

(Received 31 May 1984)

The L_3 Au edge of small evaporated gold clusters has been studied by x-ray-absorption spectroscopy at the Frascati synchrotron radiation facility. Sample discontinuity and particle size were controlled by optical transmission measurements and electron microscopy analysis. The extended x-ray-absorption fine-structure spectra showed evidence of nearest-neighbor-distance contraction, whose value reached 2.5% for the smallest clusters. The behavior of the nearest-neighbor-distance contraction versus cluster diameter agreed with a macroscopic liquid-drop model. Increases in the nearest-neighbor-distance fluctuations around the equilibrium positions were found due to the higher mobility of the surface atoms with respect to the bulk ones. The slight increase of statical disorder together with the general features of the x-ray-absorption near-edge structure spectra allowed us to exclude structural changes from the fcc bulk metal structure to the icosahedral structure, even for clusters of 50 atoms.

I. INTRODUCTION

During the last decade, the chemical and physical properties of small metal clusters have been an active area of research.[1–16] In fact the enhancement of chemical reactivity,[17] the lowering of the melting temperature,[18] and the magnetic behavior[19,20] of the metal clusters are peculiar properties widely exploited in many technological applications, among them heterogeneous catalysis.[17] Many theoretical and experimental studies have been and are being performed on the electronic and structural properties of metal clusters under different conditions such as differing chemical environment, sample preparation, size, and substrates.[1–17,21–27] Many problems are still unsolved: for instance, it is unknown if the cluster-size-dependent chemical reactivity is due to a change in their electronic or in their structural properties and how these properties depend on the sample preparation method and on the interaction with substrates.[1,17]

In this paper we report an investigation on the structural properties of Au clusters, evaporated on a weakly interacting substrate, whose average diameters range from 11 up to 60 Å.

In the past, experiments using diffraction have been made on Au clusters in order to measure the lattice parameters as a function of the cluster size.[28,29] Lattice-parameter contractions have been observed, but there is great disagreement among the numerical values obtained on clusters of same diameter: for instance, for a 35-Å cluster diameter values ranging from 0.4% to 2.7% are reported. This is due to the diffraction method which becomes less and less sensitive as the cluster size decreases.[30] In order to determine the effective amount of contractions and to check also changes in the crystallographic cluster structure,[31,32] we performed a complete structural investigation using EXAFS[33,34] (extended x-ray-absorption fine structure) and XANES[35,36] (x-ray-absorption near-edge structure).

The layout of this paper is as follows: In Sec. II we report the sample preparation; we briefly describe the details regarding their characterization using optical transmittance and electron microscopy measurements and describe the x-ray-absorption spectra. Section III contains the x-ray-absorption and EXAFS data analysis. In Sec. IV we discuss the results and their interpretation. Section V is a summary of the main results.

II. SAMPLE PREPARATION AND CHARACTERIZATION; ABSORPTION MEASUREMENTS

Cluster samples were prepared under vacuum on a 6-μm polymer film by consecutive evaporation of gold (purity=99.99%) and Mylar to achieve the optimum metal thickness for x-ray measurements.[33] The amount of Au deposited on each layer of the different samples studied is reported in Table I; the Mylar thickness was always around 200 Å. Gold and Mylar depositions were both controlled with a quartz-crystal detector.

In order to check that the multilayer samples were discontinuous, optical transmission measurements were made at normal incidence in the spectral range 0.25—2.5 μm. It is known that the transmittance spectra of discon-

TABLE I. Values of coverages (t), mean diameters (D), and diameter standard deviations (σ) of the samples studied.

t (atoms/cm^2)	D (Å)	σ (Å)
0.6×10^{15}	11.0	6.5
1.8×10^{15}	15.0	5.4
3.0×10^{15}	20.0	7.5
4.1×10^{15}	24.0	8.2
5.9×10^{15}	30.0	8.9
12.0×10^{15}	42.5	11.0
18.0×10^{15}	60.0	18.0

tinuous films, contrary to those of continuous films, generally show a wide minimum (optical conduction resonance) below the interband transitions[37] due to the free electrons in the metal particles and a high transmission in the near ir.[38] The comparison between the optical transmission spectra of our samples and of a continuous film demonstrates the sample discontinuity (Fig. 1). The distributions of cluster dimensions were determined by electron microscopy analysis (Fig. 2 and Table I).

X-ray-absorption spectra (Fig. 3) at liquid-nitrogen temperature (LNT) and at room temperature were recorded on the L_3 Au absorption edge at the Frascati National Laboratory using the wiggler photon-beam line, with typically $I=40$ mA and $E=1.5$ GeV in the storage ring and $B=18.5$ kG in the wiggler magnet.[39,40] The critical energy in this condition is 2.77 keV. The monochromator was equipped with a Si(111) channel-cut crystal and the detection of the x-ray beam was achieved by two ionization chambers filled with Kr gas.

III. EXAFS DATA ANALYSIS

The x-ray absorption spectra were analyzed using a standard procedure[41] to extract the oscillating part of the spectrum, or $\chi(k)$, given by[34]

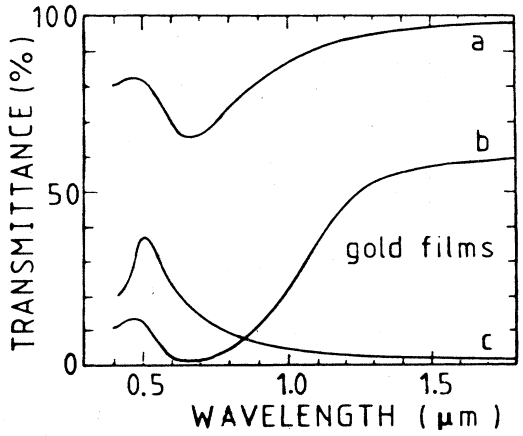

FIG. 1. Example of comparison between measured optical-transmittance spectra of different gold films: *a*, single discontinuous layer with a coverage of 18.0×10^{15} atoms/cm^2; *b*, ten discontinuous layers each having a coverage of 18.0×10^{15} atoms/cm^2; *c*, continuous film having the same total thickness of sample *b*.

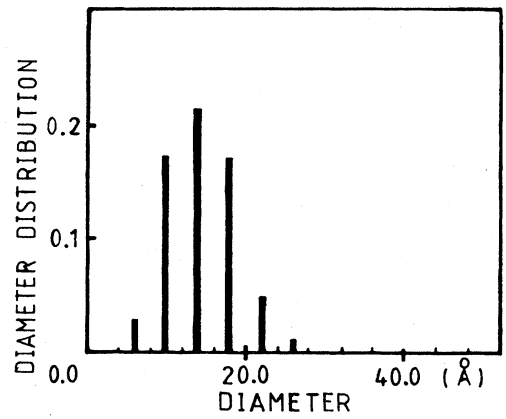

FIG. 2. Gold cluster size distribution for a coverage of 1.77×10^{15} atoms/cm^2.

$$\chi(k)=\frac{\mu_{L_3}(k)-\mu_0(k)}{\mu_0(k)},$$

where $\mu_{L_3}(k)$ is the Au L_3-shell contribution to the absorption coefficient, $\mu_0(k)$ is the atomic absorption coefficient about which $\mu_{L_3}(k)$ oscillates, and k is the photoelectron wave vector given by

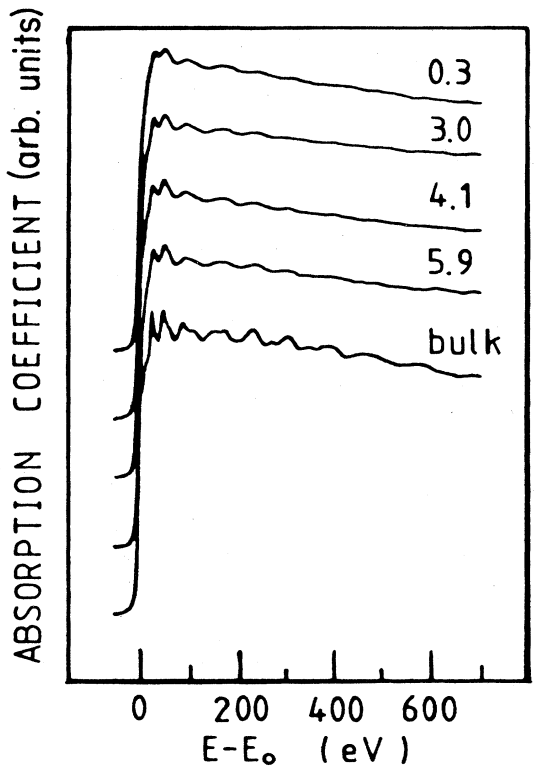

FIG. 3. Absorption coefficients at the L_3 Au edge of some of the samples studied. Coverages indicated in the figure for each sample are in units of 10^{15} atoms/cm^2. The zero of the energy has been assumed at the edge inflection point.

$$k=\left[\frac{2m(E-E_0)}{\hbar^2}\right]^{1/2},$$

where E is the incoming photon energy and E_0 is the threshold energy.

In general, there are two contributions to an L_3 edge, coming from two possible transitions: $2p\rightarrow ns$ and $2p\rightarrow nd$. It has been theoretically demonstrated and experimentally proved[42–44] that the former is only a few percent of the latter. As a consequence, the EXAFS on an L_3 edge can be well approximated by the single final-state expression of a K edge:[33]

$$\chi(k)=\sum_j \frac{S_0^2 N_j |f_j(k,\pi)| e^{-2k^2\sigma_j^2}}{kR_j^2}\sin(2kR_j+\Phi_j^{L_3}) . \quad (1)$$

In Eq. (1), R_j is the distance between the absorbing and backscattering atom, N_j is the number of the backscattering atoms in the jth shell, σ_j^2 is the mean-square fluctuation in R_j, $|f_j(k,\pi)|$ is the backscattering amplitude of the neighboring atoms, $\Phi_j^{L_3}(k)$ is the k-dependent phase shift for a d-symmetry final state, and S_0^2 is the reduction factor due to multielectron excitation. Information on the structural parameters R_j, σ_j^2, and N_j can be obtained from EXAFS spectra if the scattering functions $|f_j(k,\pi)|$ and $\Phi_j^{L_3}(k)$ are known. These functions can be transferred, from a system to another, but for $|f_j(k,\pi)|$ this is possible only provided that the two systems are chemically similar.[45,46] The gold phase shift and backscattering amplitude have been obtained analyzing the EXAFS spectrum of a 4-μm Au foil at LNT [Fig. 4(a)]. The Fourier transform (FT) of this EXAFS spectrum [Fig. 4(b)] shows several peaks, corresponding to the different coordination shells shifted from the crystallographic values by a quantity due to the presence of the phase term in $\chi(k)$.[47] We note that the first peak in real space is split due to the highly nonlinear Au phase [Fig. 5(a)] and to the oscillatory behavior of the backscattering amplitude [Fig. 5(b)]. The positions and relative intensities of these two split components depend on the FT conditions as can be seen comparing the bulk FT of Figs. 4(b) and 6. For this reason we transformed all the cluster EXAFS spectra under the same conditions (Fig. 6).

It is evident that as the film thickness decreases there is a shift of the FT main peak towards smaller R. Table II reports the nearest-neighbor (NN) distance values obtained.

Information about the mean coordination numbers and the Debye-Waller factors were obtained from data analysis in k space. The inverse Fourier transform of the first FT double peak allows one to select the contribution to the $\chi(k)$ due only to the first coordination shell. In this way it is possible to analyze separately the amplitude function

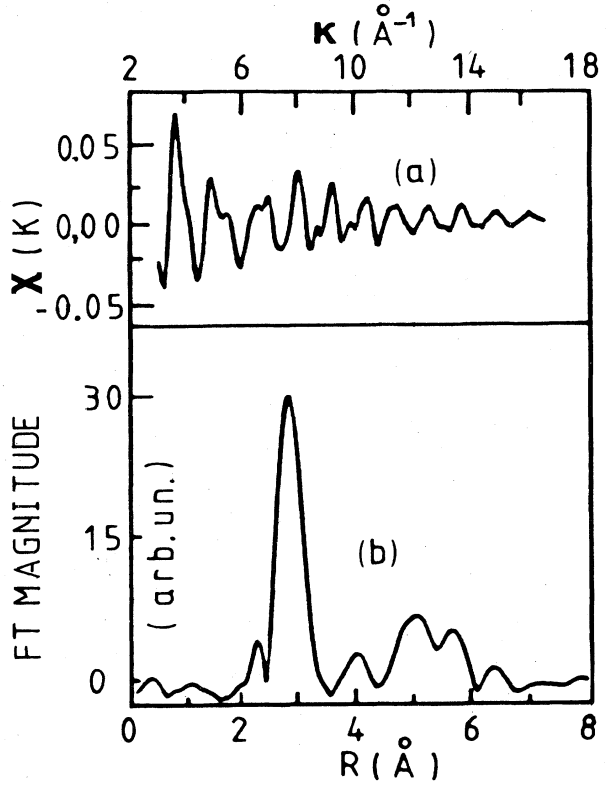

FIG. 4. (a) EXAFS spectrum of Au bulk at 77 K. (b) Fourier transform of bulk EXAFS spectrum in the k range 3–16 Å^{-1} with a Gaussian window function and a k^3 weight.

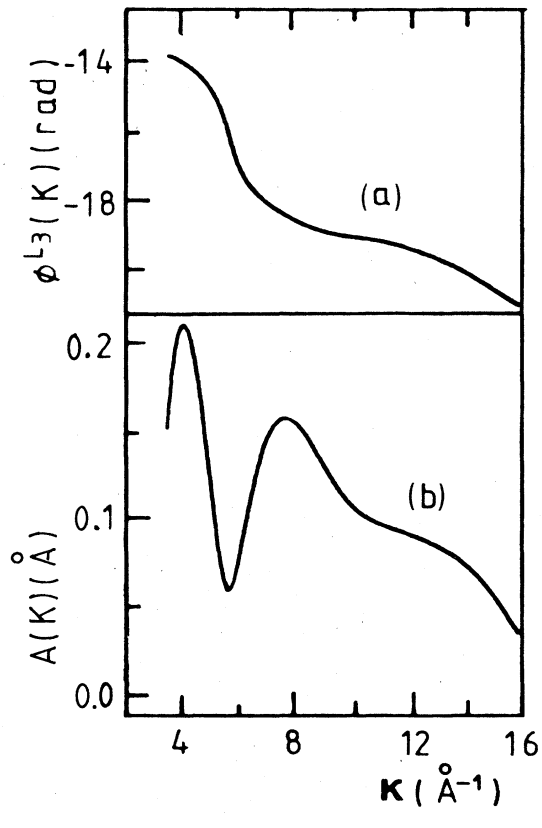

FIG. 5. (a) Phase and (b) amplitude functions for Au bulk at 77 K, obtained backtransforming the region 2.1–3.5 Å of Fig. 4(b).

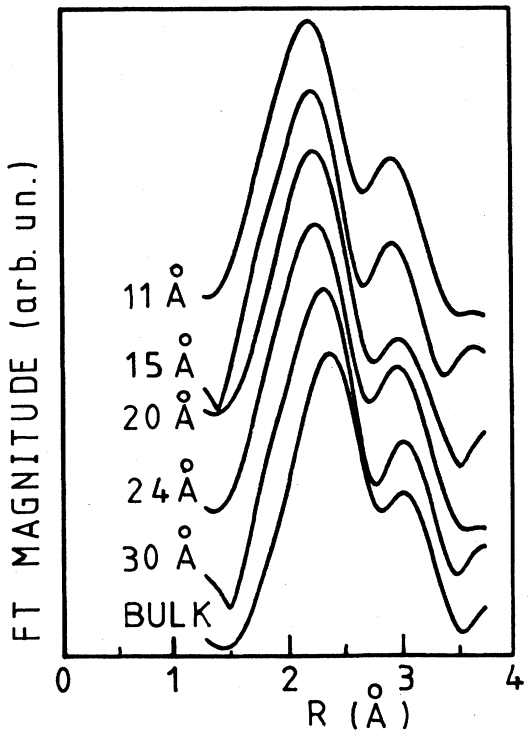

FIG. 6. Fourier transforms of the films and bulk EXAFS spectra. The transformations are now in the range 3–11 Å^{-1} with k^1 weight and a Gaussian window function.

$$A(k)=\frac{S_0^2 N}{R^2}e^{-2k^2\sigma^2}|f(k,\pi)|\ ,$$

and the "total" phase function[48]

$$\Pi(k)=2kR+\Phi^{L_3}\ .$$

Plotting the function

$$\ln\left[\frac{A_{\text{cluster}}}{A_{\text{bulk}}}\right]$$

versus k^2, a straight line is obtained[48] whose slope is given by

$$-2(\sigma^2_{\text{cluster}}-\sigma^2_{\text{bulk}})\ ,$$

and whose extrapolation to $k^2=0$ is

$$\ln\left[\frac{(N/R^2)_{\text{cluster}}}{(N/R)_{\text{bulk}}}\right]\ .$$

The values of N and σ^2 obtained using this approach are reported in Table III. We note that as the cluster size decreases the mean coordination number decreases and the cluster disorder factor increases.

It is also possible to obtain the NN distances in k space[49] using the following relation:

$$R_{\text{cluster}}=\frac{\Pi_{\text{cluster}}(k)-\Phi^{L_3}(k)}{2k}\ .$$

The values so obtained are just like the ones obtained in R space (Table II).

Great attention was given to the possible presence of asymmetry effects in the radial distribution function (RDF), which can result in apparent NN contractions.[50] The origin of such effects can be dynamical or static.[51–53] We can exclude the presence of dynamical asymmetry effects because the cluster total phase obtained by EXAFS data analysis was found to be independent of temperature. Besides, the asymmetry effects on Pt/SiO_2 clusters have have been experienced to be negligible up to 500 K.[54]

Presence of asymmetry static effects can be excluded *a posteriori* since the analysis with a Gaussian function gives a decrease in the NN distances, a decrease of the coordination numbers, and an increase of the Debye-Waller factors, all of which are completely explained by the increased surface-to-volume ratio.

IV. DISCUSSION

A. Interatomic-distance results

Figure 7 shows the NN distance contractions found as a function of the inverse of mean cluster diameter. These values clearly show a contraction in the NN distances up to 2.5%. We believe that these results obtained by EXAFS do not have the same kind of limitations that the diffraction results have. EXAFS, in fact, is able to mea-

TABLE II. Values of the nearest-neighbor distances of Au clusters obtained from Fourier spectra and from k-space analysis. The Fourier values have been obtained adding the phase-shift contribution $\delta=0.51$ Å, calculated from the bulk spectrum, to the positions of sample Fourier spectra maxima.

D (Å)	R_{Fourier} (Å) (±0.02 Å)	$R(k)$ (Å) (±0.01 Å)
11.0	2.82	2.81
15.0	2.83	2.82
20.0	2.84	2.83
24.0	2.85	2.85
30.0	2.86	2.85
42.5	2.87	2.86
60.0	2.87	2.87

TABLE III. Coordination numbers (N) and Debye-Waller factors (σ^2) at 300 K and 77 K obtained from analysis in k space. The bulk σ_B^2 at 77 K has been assumed equal to 1.7×10^{-3} Å^2 according to Ref. 59.

D (Å)	N (±10%)	σ^2 (Å^2) 300 K (±20%)	σ^2 (Å^2) 77 K (±20%)
bulk	12.0	4.9×10^{-3}	1.7×10^{-3}
42.5	11.0	6.7×10^{-3}	2.4×10^{-3}
30.0	10.6	7.0×10^{-3}	2.6×10^{-3}
24.0	10.0	8.6×10^{-3}	4.2×10^{-3}
20.0	9.6	10.7×10^{-3}	5.5×10^{-3}
15.0	9.4	10.0×10^{-3}	

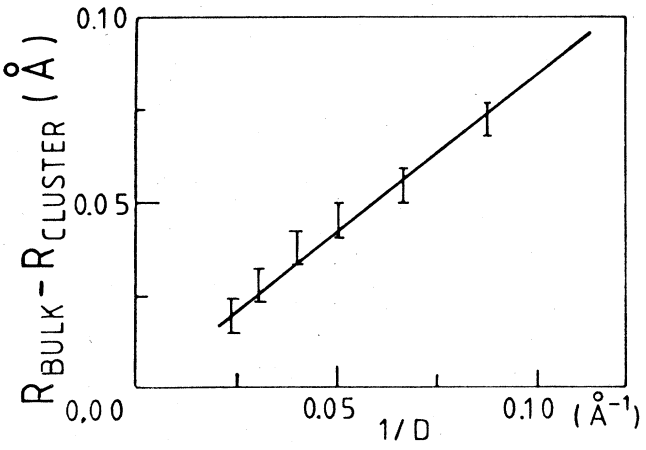

FIG. 7. Plot of nearest-neighbor-distance contraction vs the inverse of the cluster mean diameter. The straight line drawn is the data mean-square linear fit.

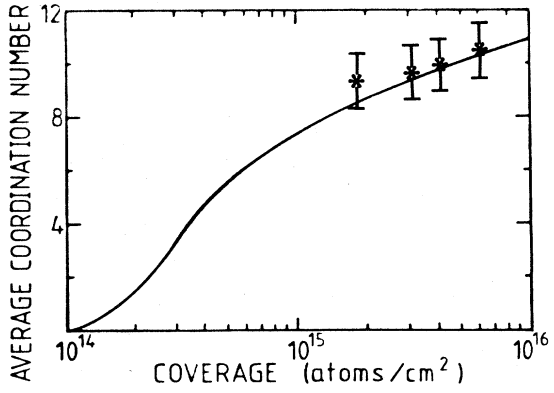

FIG. 8. Behavior of the average coordination number versus coverage for gold on carbon (solid line) (Ref. 1). The asterisks (*) are experimental data obtained for our gold clusters on Mylar.

sure also a dimer interatomic distance.[16] From a macroscopic point of view the contraction of the NN distances is explained in terms of surface stress due to the high value of the surface to volume ratio in the clusters. For a liquid drop model,[55] the contraction ΔR due to surface stress f is given by

$$\Delta R = -\tfrac{4}{3} K R_b f \frac{1}{D} ,$$

where K is the bulk compressibility, R_b is the metal bulk NN distance, and D is the mean cluster diameter. The data in Fig. 7 clearly show a linear dependence versus $1/D$. From this analysis we argue that the macroscopic approximation is surely valid for cluster sizes greater than 11 Å.

Our results are in contrast with recent EXAFS results on metal clusters in catalytic systems where the NN distances are similar to the bulk ones within 0.02 Å.[12–14,56] On the other hand, they agree with those on Cu and Ni clusters prepared under vacuum evaporation.[15,24] These two different behaviors are due to the different metal-substrate interactions. It has been experimentally demonstrated that when there are no interactions between metals and substrates, as in the case of metal clusters in rare-gas matrices, contractions are present.[16,57] In our case the interactions between clusters and substrates are certainly weak, as will be shown in the following.

B. Coordination-number results

Figure 8 shows the experimental behavior of the mean coordination number reported by Mason[1] for gold on carbon versus coverage together with our EXAFS results. We want to stress that our data are the first direct determinations of coordination numbers in evaporated metal clusters. The agreement observed demonstrates that Mylar, like carbon, is a weakly interacting substrate for metal clusters and states again that there are no asymmetry effects. In fact, another main effect of an asymmetric RDF is a dramatic lowering of the coordination numbers.[50]

C. Debye-Waller–factor results

The increase in cluster disorder is mainly dynamical in the origin. The behavior of σ^2 versus T^2 is reported in Fig. 9. In the Debye correlated approximation[58]

$$\sigma^2(T) = \sigma_S^2 + \frac{6h^2}{mk_B\Theta_D}\left[\frac{1}{4}+\left[\frac{T}{\Theta_D}\right]^2 D_1\right] - \frac{6h^2}{mk_B\Theta_D}\left[\frac{1-\cos(q_D R_j)}{2(q_D R_j)^2}+\left[\frac{T}{\Theta_D}\right]^2 D_1\right], \quad (2)$$

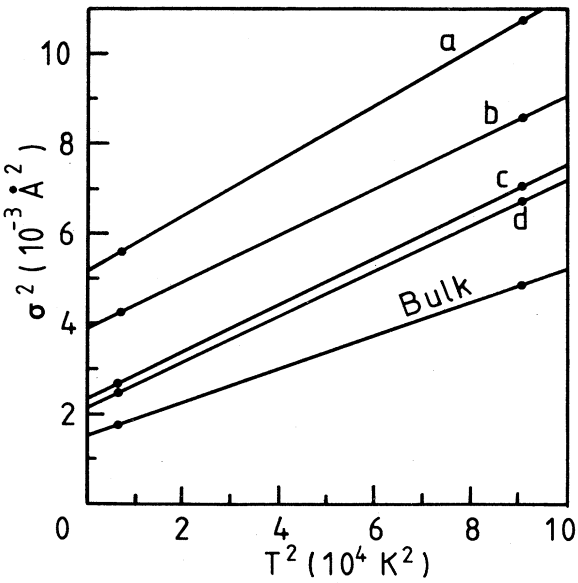

FIG. 9. Plot of Debye-Waller factors vs T^2 for some of the samples studied: *a*, 20-Å clusters; *b*, 24-Å clusters; *c*, 30-Å clusters; and *d*, 42.5-Å clusters. The bulk σ_B^2 at 77 K has been assumed equal to 1.7×10^{-3} Å^2, according to Ref. 59.

where σ_S^2 is the statical contribution to the disorder, Θ_D and q_D, respectively, are the Debye temperature and wave vector, and k_B is the Boltzmann constant. D_1 is the slowly varying function:

$$D_1\left[\frac{\Theta_D}{T}\right]=\int_0^{\Theta_D/T}\frac{x}{e^x-1}dx \ .$$

The use of the Debye approximation for gold is justified since it has been experimentally demonstrated that in metals the Debye approximation is valid up to twice the Debye temperature ($\Theta_D^{\text{bulk}}=165$ K).[59] The two expressions in square brackets of Eq. (2) are due to the total and to the correlated motion, respectively. It has been demonstrated[58] that for a fcc metal the correlated motion is about 0.35 times the total motion for $T\geq 0.55\Theta_D$, which is the range of temperature of interest. Equation (4) can therefore be approximated by

$$\sigma^2(T)=\sigma_S^2+0.65\frac{6h^2}{mk_B\Theta_D}\left[\frac{1}{4}+\left[\frac{T}{\Theta_D}\right]^2 D_1\right] .$$

In Fig. 9, the σ^2 values obtained by extrapolating the straight line to $T=0$ are due to the static (σ_S^2) and dynamical ($0.98h^2/mk\Theta_D$) factors while the slopes are only due to the dynamical disorder. In Table IV we report the values of the cluster Debye temperatures as deduced from slopes.

The decrease in cluster Debye temperatures are again due to the greater number of surface atoms. Low-energy electron diffraction (LEED) measurements have indeed shown higher surface-atom mobility with respect to the bulk and have determined surface Debye temperatures for different Miller planes.[60] Such Debye temperatures are always lower than the bulk one. As a first approximation we assume that the cluster Debye temperature approach the surface one, averaged over all possible surfaces, as the cluster sizes decrease. This average, using data[60] from literature, gives, for gold,

$$\Theta_D^{\text{cluster}}=135 \text{ K}\approx 0.8\Theta_D^{\text{bulk}} ,$$

which is in good agreement with data of Table IV.

To evaluate the statical disorder we subtracted from $T^2=0$ cluster σ^2 values obtained from Fig. 9, with the dynamical contribution given by

$$\frac{0.98h^2}{mk\Theta_D^{\text{cluster}}} .$$

Table IV reports the σ_S^2 values obtained. The increase in static disorder is only partially due to the cluster-size distribution inside each sample. In fact, for a film containing clusters of 20 Å, and using the values of Tables I and II for the cluster-size distributions and the NN distance values, respectively, we calculated a static disorder factor of 10^{-3} Å^2, which is smaller than the value reported in Table IV.

Moreover, the slight static disorder found cannot be ascribed to structural changes to icosahedra. This disagrees with thermodynamical considerations which predict a structural transition from fcc to icosahedra for clusters containing less than 150 atoms.[31,61,62] In the icosahedra the first fcc shell is split into two shells centered at distances R_{I} and R_{II} and related by

$$R_{\text{I}}=1.05R_{\text{II}} .$$

Such a system would have a $\sigma_S^2=0.012$ Å^2, which is much greater than the values observed.

In order to exclude completely the presence of icosahedra in our samples, we performed fits to the inverse Fourier transform spectra using a fcc model and an icosahedral model.[63] Only using a single-shell fcc model were good fits obtained for all samples.

The question of whether the structure is still fcc up to the second and third shells can be fully clarified from the XANES spectra,[35,36] shown in Fig. 10, which have a typical fcc shape in going from the bulk to the 11-Å cluster. The two peaks labeled *b* and *c* have indeed been shown to

TABLE IV. Clusters, Debye temperature (Θ_D), and statical disorder factors (σ_S^2).

D (Å)	Θ_D (K)	σ_S^2 (Å^2)
42.5	150	0.80×10^{-3}
30.0	148	0.95×10^{-3}
24.0	148	2.55×10^{-3}
20.0	140	3.80×10^{-3}

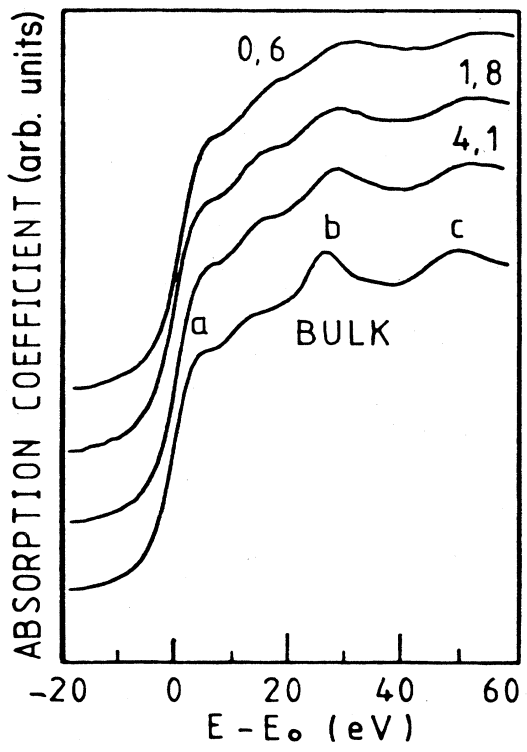

FIG. 10. XANES spectra for some of the samples studied. Coverages indicated are in units of 10^{15} atoms/cm^2; the zero of the energy has been assumed at the edge inflection point.

emerge from only fcc structures ordered up to the third shell.[64] It can be seen that as the cluster size decreases there is a shift to higher energies and a broadening of the XANES peaks. The former is due to the shortening of the lattice parameters,[65] while the latter is a consequence of both the cluster-size distribution inside each sample and of the different weight of the second- and third-shell contributions to the spectra for different samples. A quantitative analysis of the XANES data will be published elsewhere.

V. CONCLUSIONS

In conclusion, we have shown that in evaporated Au metal clusters on a weakly interacting substrate the cluster structure is still fcc, like the bulk, but there is a contraction of the NN distance. We quantitatively determined this contraction for cluster sizes ranging from 11 up to 60 Å. We measured the rms deviations of atoms around their positions and found that they are mainly dynamical in character. We deduced the Debye temperatures of the clusters studied, which were in excellent agreement with LEED data. It is nonetheless our opinion that many questions remain to be solved, in particular, the nature of the cluster-substrate interaction, before we will have a generally consistent picture of small-cluster behavior and understand the discrepancies existing in the literature.

ACKNOWLEDGMENTS

The authors are grateful to the machine staff of the Laboratori Nazionali di Frascati and to the members of the synchrotron radiation group for their collaboration during the measurements. Thanks are due Dr. P. Rosa for the electron microscopy analysis, performed at the Istituto Superiore di Sanita' of Rome. The fruitful discussions with Dr. L. Incoccia have been invaluable during all stages of this work.

[1]M. G. Mason, Phys. Rev. B **27**, 748 (1983).
[2]M. G. Mason, L. J. Gerenser, and S. T. Lee, Phys. Rev. Lett. **39**, 288 (1977).
[3]R. C. Baetzold, J. Chem. Phys. **68**, 555 (1978).
[4]J. Colbert, A. Zangwill, Myron Strongin, and S. Krummacher, Phys. Rev. B **27**, 1378 (1983).
[5]C. Battistoni, G. Mattogno, R. Zanoni, and L. Naldini, J. Electron Spectrosc. Relat. Phenom. **28**, 23 (1982).
[6]K. S. Liang, W. R. Salamek, and L. A. Aksay, Solid State Commun. **19**, 329 (1976).
[7]G. O. Ozin and F. Hugues, J. Phys. Chem. **87**, 94 (1983).
[8]R. C. Baetzold, M. G. Mason, and J. H. Hamilton, J. Chem. Phys. **72**, 366 (1980).
[9]W. F. Egelhoff, Jr. and G. G. Tibbets, Phys. Rev. B **19**, 5028 (1979).
[10]H. Roulet, J. M. Mariot, G. Dufour, and C. F. Hague, J. Phys. F **10**, 1025 (1980).
[11]S. R. Sashital, J. B. Cohen, R. L. Burwell, Jr., and J. B. Butt, J. Catal. **50**, 479 (1977).
[12]J. H. Sinfelt, G. H. Via, F. W. Lytle, and R. B. Greegor, J. Chem. Phys. **75**, 5527 (1981).
[13]J. H. Sinfelt, G. H. Via, and F. W. Lytle, J. Chem. Phys. **76**, 2779 (1982).
[14]G. H. Via, J. H. Sinfelt, and F. W. Lytle, J. Chem. Phys. **71**, 690 (1979).
[15]G. Apai, J. Hamilton, J. Stohr, and A. Thompson, Phys. Rev. Lett. **43**, 165 (1979).
[16]H. Purdum, P. A. Montano, G. K. Shenoy, and T. Morrison, Phys. Rev. B **25**, 4412 (1982).
[17]J. Sinfelt, Rev. Mod. Phys. **51**, 569 (1979).
[18]J. Q. Broughton and L. V. Woocock, J. Phys. C **11**, 2743 (1978).
[19]J. L. Dormann, Rev. Phys. Appl. **16**, 275 (1981).
[20]J. L. Dormann, D. Fiorani, J. L. Tholence, and C. Sella, J. Magn. Magn. Mater. **35**, 117 (1983).
[21]W. F. Egelhoff, Jr. and G. G. Tibbetts, Phys. Rev. B **19**, 5028 (1979).
[22]J. F. Hamilton and P. C. Logel, Thin Solid Films **16**, 49 (1973).
[23]J. F. Hamilton and P. C. Logel, Thin Solid Films **23**, 89 (1974).
[24]M. De Crescenzi, P. Picozzi, S. Santucci, C. Battistoni, and G. Mottango, Solid State Commun. (to be published).
[25]M. Boudart, A. Aldag, J. E. Benson, N. A. Dougharty, and C. G. Harkins, J. Catal. **6**, 92 (1966).
[26]W. F. Taylor, D. J. C. Yates, and J. H. Sinfelt, J. Am. Chem. Soc. **86**, 2966 (1964).
[27]P. Schoubye, J. Catal. **14**, 238 (1969).
[28]C. Berry, Phys. Rev. B **88**, 596 (1952).
[29]H. J. Wasserman and J. S. Vermaack, Surf. Sci. **22**, 164 (1970).
[30]C. L. Briant and J. J. Burton, Surf. Sci. **51**, 345 (1975).
[31]M. B. Gordon, F. Cyrot-Lackmann, and M. C. Desjonqueres, Surf. Sci. **80**, 159 (1980).
[32]B. Moraweck and A. J. Renouprez, Surf. Sci. **106**, 35 (1981).
[33]P. A. Lee, P. H. Citrin, P. Eisenberger, and B. M. Kincaid, Rev. Mod. Phys. **53**, 769 (1981).
[34]E. A. Stern, D. E. Sayers, and F. W. Lytle, Phys. Rev. B **11**, 4836 (1975).
[35]M. Belli, A. Scafati, A. Bianconi, S. Mobilio, L. Palladino, A. Reale, and E. Burattini, Solid State Commun. **35**, 355 (1981).
[36]J. B. Pendry, in *EXAFS and Near Edge Structure,* edited by A. Bianconi, L. Incoccia, and S. Stipcich (Springer, Berlin, 1983), p. 4.
[37]J. P. Marton and J. R. Lemon, Phys. Rev. B **4**, 271 (1971).
[38]S. Normann, T. Andersson, C. G. Granqvist, and O. Hundrey, Phys. Rev. B **18**, 674 (1978).
[39]R. Barbini, M. Bassetti, M. E. Biagini, R. Boni, A. Cattoni, V. Chimenti, S. De Simone, B. Dulach, S. Faini, S. Guiducci, A. U. Luccio, M. A. Preger, C. Sanelli, M. Serio, S. Tazzari, F. Tazzioli, M. Vescovi, G. Vignola, A. Vitali, E. Burattini, N. Cavallo, M. Foresti, C. Mencuccini, E. Pancini, P. Patteri, R. Rinzivillo, U. Troya, G. Dalba, F. Ferrari, P. Fornasini, A. Jackson, and J. Worgan, Riv. Nuovo Cimento **4** (1981).
[40]E. Burattini, A. Reale, E. Bernieri, N. Cavallo, A. Morone, M. R. Masullo, R. Rinzivillo, G. Dalba, P. Fornasini, and C. Mencuccini, Nucl. Instrum. Methods **208**, 91 (1983).
[41]S. Mobilio, F. Comin, and L. Incoccia, Laboratori Nazionali di Frascati Internal Report No. 82/19 (NT), 1982 (unpublished).

[42]F. W. Lytle, D. E. Sayers, and E. A. Stern, Phys. Rev. B **15**, 2426 (1977).
[43]B. K. Teo and P. A. Lee, J. Am. Chem. Soc. **101**, 2815 (1979).
[44]P. Rabe, G. Tolkien, and A. Werner, J. Phys. C **12**, 899 (1979).
[45]P. H. Citrin, P. Eisenberger, and B. M. Kincaid, Phys. Rev. Lett. **36**, 1346 (1976).
[46]E. A. Stern, B. A. Bunker, and S. M. Heald, Phys. Rev. B **21**, 5521 (1980).
[47]D. E. Sayers, E. A. Stern, and F. W. Lytle, Phys. Rev. Lett. **35**, 584 (1975).
[48]G. Martens, P. Rabe, N. Schwentner, and A. Werner, Phys. Rev. B **17**, 1481 (1978).
[49]P. Rabe, Jpn. J. Appl. Phys. **17**, 22 (1978).
[50]P. Eisenberger and G. S. Brown, Solid State Commun. **29**, 481 (1979).
[51]R. Haensel, P. Rabe, G. Tolkien, and A. Werner, in *Liquid and Amorphous Metals,* Proceedings of the NATO Advanced Study Institute, edited by E. Luscher (Reidel, Dordrecht, 1980).
[52]M. De Crescenzi, A. Balzarotti, F. Comin, L. Incoccia, S. Mobilio, and N. Motta, Solid State Commun. **37**, 921 (1981).
[53]S. Mobilio and L. Incoccia, Nuovo Cimento **30**, 846 (1984).
[54]E. C. Marques, D. R. Sandstrom, F. W. Lytle, and R. B. Greegor, J. Chem. Phys. **77**, 1027 (1982).
[55]C. W. Mays, J. S. Vermaak, and D. Kuhlmann-Wilsorf, Surf. Sci. **12**, 134 (1968).
[56]P. Lagarde, T. Murata, G. Vlaic, E. Freund, H. Dexpert, and J. P. Bounouville, J. Catal. **84**, 333 (1983).
[57]P. A. Montano and G. K. Shenoy, Solid State Commun. **35**, 53 (1980).
[58]G. Beni and P. M. Platzmann, Phys. Rev. B **14**, 9514 (1976).
[59]R. B. Greegor and F. W. Lytle, Phys. Rev. B **20**, 4902 (1979); E. Sevillano, H. Meuth, and J. J. Rehr, Phys. Rev. B **20**, 4908 (1979).
[60]D. P. Jackson, Surf. Sci. **43**, 431 (1974).
[61]J. P. Borel, Surf. Sci. **106**, 1 (1981).
[62]J. J. Burton, Catal. Rev. (Sci. Eng.) **9**, 209 (1974).
[63]The Cernlib program MINUIT was used for least-mean-squares fitting.
[64]G. N. Greaves, P. G. Graham, G. Diakun, and P. Quin, Nature **294**, 139 (1981).
[65]C. R. Natoli, in *EXAFS and Near Edge Structure,* Ref. 36, p. 43.